



Synergetic–Complementary Use of Industrial Solid Wastes to Prepare High-Performance Rapid Repair Mortar

Jingwei Li^{*†}, Dong Xu[†], Xujiang Wang, Kun Wang and Wenlong Wang

National Engineering Laboratory for Reducing Emissions From Coal Combustion, Engineering Research Center of Environmental Thermal Technology of Ministry of Education, Shandong Key Laboratory of Energy Carbon Reduction and Resource Utilization, School of Energy and Power Engineering, Shandong University, Jinan, China

OPEN ACCESS

Edited by:

Lijie Guo,
Beijing General Research Institute of
Mining and Metallurgy, China

Reviewed by:

Jiaqi Li,
University of California, Berkeley,
United States
Shiqi Dong,
University of California, Los Angeles,
United States

*Correspondence:

Jingwei Li
ljw@sdu.edu.cn

[†]These authors have contributed
equally to this work

Specialty section:

This article was submitted to
Structural Materials,
a section of the journal
Frontiers in Materials

Received: 10 October 2021

Accepted: 02 November 2021

Published: 03 December 2021

Citation:

Li J, Xu D, Wang X, Wang K and
Wang W (2021)
Synergetic–Complementary Use of
Industrial Solid Wastes to Prepare
High-Performance Rapid
Repair Mortar.
Front. Mater. 8:792299.
doi: 10.3389/fmats.2021.792299

With the vigorous development of infrastructure engineering, there are growing demands for high-performance rapid repair mortar, especially those using environmental-friendly and low-carbon cementitious materials. Hereupon, this work explored an innovative approach for rapid repair mortar preparation using solid waste-based calcium sulfoaluminate cement. The calcium sulfoaluminate cement was first prepared via synergetic–complementary use of industrial solid wastes and then adopted to prepare rapid repair mortar by proportionally mixing with standard sand and four additives (i.e., polycarboxylate superplasticizer, lithium carbonate, boric acid, and latex powder). The mechanistic analysis indicated that the four additives comprehensively optimized the mechanical strengths, fluidity, and setting time of rapid repair mortar by adjusting the hydration process of calcium sulfoaluminate cement. The test results showed that the 2-h compressive and flexural strength, and 1-day bonding strength of the prepared rapid repair mortar were 32.5, 9.2, and 2.01 MPa, respectively, indicating excellent early-age mechanical performance. In addition, the 28-day compressive and flexural strengths of the rapid repair mortar reached 71.8 and 17.7 MPa. Finally, a life cycle assessment and economic analysis indicated that this approach achieved environmental-friendly utilization of industrial solid wastes, and cost-effective and energy-saving natures, which supports current trends towards a circular economy and green sustainable development.

Keywords: rapid repair mortar, sulfate-based cements, industrial wastes, recycling, environmental friendliness

INTRODUCTION

Recently, large-scale infrastructure engineering such as railways, highways, bridges, water conservancy, and buildings are developing vigorously in China, and the number of these engineering infrastructures is more than that in foreign countries combined. Statistically, the annual output of concrete has reached more than 2.5 billion m³ in China (Chinaconcretes., 2020). However, the concrete structures can be damaged due to natural disasters, climate change, or continuous load, which affect the safety and normal of the facilities (Han et al., 2015; Song et al., 2018; Feng et al., 2019). Therefore, the maintenance and repair industries of concrete structures and facilities are likely to develop rapidly, and there will be massive demands for rapid repair mortars (RRMs) with properties of fast hardening, high fluidity, and early compressive

strength (i.e., ≥ 20 MPa in 2–4 h) (Moffatt and Thomas, 2017). For decades, ordinary Portland cement (OPC) has been commonly used as a cementing material for RRM preparation (Feng et al., 2019; Phoo-ngernkham et al., 2019). However, traditional OPC production consumes massive resources and energy, and contributes up to $\sim 9\%$ global anthropogenic CO_2 emissions and $\sim 7\%$ primary energy consumption (Huynh et al., 2018; Li et al., 2020). Hence, there are growing demands for replacing OPC with eco-friendly and low-carbon alternatives for the sake of energy and environment sustainability (Gartner and Sui, 2018; Juenger et al., 2019).

Calcium sulfoaluminate (CSA) cement features high early strength, low permeability, rapid setting, and slight expansion properties, which are primarily attributed to the rapid crystallization of ettringite ($3\text{CaO} \cdot \text{Al}_2\text{O}_3 \cdot 3\text{CaSO}_4 \cdot 32\text{H}_2\text{O}$), produced by the hydration of the key mineral, ye'elimite ($3\text{CaO} \cdot 3\text{Al}_2\text{O}_3 \cdot \text{CaSO}_4$) (Telesca et al., 2014; Du et al., 2021). Researchers have found that CSA cement is very suitable as the cementing material for RRM preparation (Zhang J. et al., 2018; Long et al., 2019; Yeung et al., 2019). Moffatt and Thomas (2017) prepared RRM by blending 30% CSA cement with 70% OPC as the cementing material, and achieved a compressive strength of 22 MPa at 3 h. Shi et al. (2021) also prepared RRM using CSA cement, and the flexural and compressive strengths at 1 day reached ~ 7 and ~ 36 MPa. Furthermore, CSA cement is regarded as a green cement category because of its low calcination temperature ($\sim 1,250^\circ\text{C}$) and low carbon dioxide emissions (Benhelal et al., 2013; Ren et al., 2017a).

However, the annual production of CSA cement is only several million tons worldwide (Ren et al., 2017a). Traditional raw materials to prepare CSA-based cements include high-grade bauxite, natural gypsum, and limestone, which lead to high production costs and significantly restrict its large-scale application (Ren et al., 2017b), in particular, in concrete rapid repair. Researchers tried to use industrial solid wastes as substitute raw materials for CSA cement preparation. Wang et al. (2013) successfully prepared high-performance CSA cement by synergistically using low-priced industrial solid wastes, such as red mud, desulfurization gypsum, aluminum dust, and carbide slag. A comparative life cycle assessment of CSA clinker production derived from industrial solid wastes and natural raw materials by Ren et al. (2017) showed that the total environmental burden could be reduced by 38.62% with the comprehensive waste utilization compared with the traditional process. In addition, the solid waste-based CSA cement (WCSA) exhibited a good immobilization ability on heavy metals introduced from industrial solid wastes (Yao et al., 2020). Collectively, the synergistic utilization of solid waste not only can prepare high-performance CSA cement, but also has great environmental benefits and reduces the production costs. Furthermore, some researchers verified the feasibility of preparing green building materials, i.e., ready-to-use low-density foamed concrete (Yao et al., 2019), construction 3D printing material (Shahzad et al., 2020), lightweight porous concrete (Yang et al., 2021), and foamed concrete for road embankment (Ge et al., 2020). However, there are few studies

that have explored the combination of WCSA and RRM preparation.

This paper proposes an innovative, technical approach for RRM preparation with WCSA as the primary cementing material. The WCSA was first prepared by the synergetic-complementary use of four types of bulk industrial solid wastes, and was then mixed with standard sand and four additives to prepare RRM. The compressive and flexural strengths, bonding strength, and fluidity of the prepared RRM were tested. The effects of the four additives on the hydration and mechanical properties of the prepared RRM were studied. Finally, the environmental impact and economics of this approach were assessed by both a life cycle assessment and economic analysis. This paper may provide a promising pathway to realize the preparation of high-performance solid waste-derived RRM and synergetic treatment of industrial solid wastes, which is in line with current trends towards green industrial chain.

MATERIALS AND METHODS

Materials

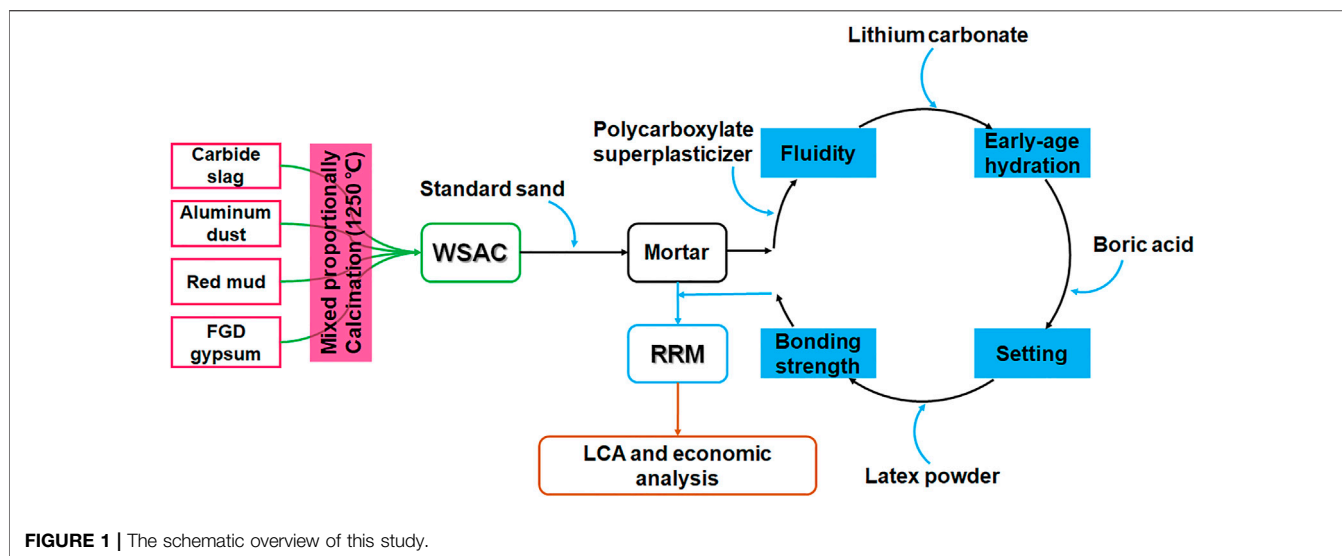
To prepare WCSA clinker, four kinds of industrial solid wastes were used with complementary matching of their ingredients. Carbide slag was sampled from the Tai'an Jiepu Technology Science and Technology Ltd. (Tai'an, China); aluminum dust was sampled from Xinfu Group (Liaocheng, China); red mud was sampled from Xinfu Group (Liaocheng, China); flue gas desulfurization (FGD) gypsum was sampled from Liaocheng Coal-fired Power Plants (Liaocheng, China). The chemical compositions and x-ray diffraction (XRD) patterns for the raw materials are provided in **Supplementary Table S1** and **Supplementary Figure S1**, respectively. Standard sand was used as the aggregate for RRM. Four kinds of additives, including polycarboxylic acid water reducer, lithium carbonate, boric acid, and dispersible latex powder, were used to adjust the hydration characteristics of RRM, i.e., fluidity, setting time, and mechanical strengths.

Experimental Procedure

The schematic overview of this study is shown in **Figure 1**. The above-mentioned industrial solid waste materials were proportionally mixed based on the following three modulus values in **Eqs 1–3**. The three modulus values were set as $C_m = 0.98$, $P = 1.85$, and $N = 3.09$, and the corresponding proportion of solid wastes is provided in **Supplementary Table S2**. The mixture of solid waste materials was caked and calcined at $1,250^\circ\text{C}$ (holding 30 min) to prepare the WCSA clinker. Then, the clinker was mixed with 5 wt% anhydrous gypsum, ground together, to prepare WCSA.

$$C_m = \frac{\text{CaO} - 0.7\text{TiO}_2}{1.87\text{SiO}_2 + 0.73(\text{Al}_2\text{O}_3 - 0.64\text{Fe}_2\text{O}_3) + 1.40\text{Fe}_2\text{O}_3} \quad (1)$$

$$P = \frac{\text{Al}_2\text{O}_3}{\text{SO}_3} \quad (2)$$



$$N = \frac{\text{Al}_2\text{O}_3}{\text{SiO}_2} \quad (3)$$

The prepared WCSA was mixed with standard sand at a weight ratio of 1:1 and then the mixture was blended with water at a water-to-binder ratio (W/B) of 0.28. Different amounts of the four additives were added into the mortar to adjust its hydration characteristics one by one: (i) polycarboxylate superplasticizer was added to adjust the fluidity at a low W/B ratio (Li et al., 2021; Tian et al., 2019), (ii) lithium carbonate was added to improve the early-age compressive and flexural strengths (Zhang Y. et al., 2018), (iii) boric acid was added to adjust the setting time (Cau Dit Coumes et al., 2017a), and (iv) dispersible latex powder was added to improve the bonding strength (Shi et al., 2021). With the optimized amounts of additives, the WCSA-based RRM was successfully prepared.

Analytical Methods

The compressive and flexural strengths of the prepared RRM were tested according to International Standard ISO 679-2009 “Cement - Test methods - Determination of strength”^[24]. The prepared RRM was mixed with water at a water-to-binder ratio of 0.28, and then stirred using a mixer. After stirring, the mortar was cast into 40 mm × 40 mm × 160 mm molds and de-molded after 24 h. The de-molded samples were cured at 95% humidity and 20 ± 2°C. The compressive and flexural strengths of the cured samples were tested using an electronic universal testing machine (YAW-300C; Zhongluchang Co., Ltd., China) after 2-h, 1-day, 3-day, and 28-day curing ages. The compressive and flexural strengths (1 day, 3 days, and 28 days) of the prepared WCSA were also tested according to International Standard ISO 679-2009, and the mass ratio of WCSA:standard sand:water was 1: 3: 0.5.

The bonding strength of the prepared RRM was tested according to Chinese Industry standard JC/T 2381-2016 “Repairing mortar, 2016”^[25]. A base mortar with dimensions of 70 mm × 70 mm × 20 mm was prepared using OPC and cured

at 95% humidity and 20 ± 2°C for 28 days. A forming frame was placed on the base mortar and then the RRM slurry was poured into the forming frame and cured at 95% humidity and 20 ± 2°C. The bonding strength was determined after 1-day curing age.

The fluidity test for the prepared RRM was conducted on the basis of Chinese national standard GB/T 2419-2005 “Test method for fluidity of cement mortar”^[26]. The RRM slurry was added to truncated cone dies, where the round die was slowly filled, allowing the slurry to flow undisturbed and freely before it eventually stopped. Then, measurements of the largest diameter of the slurry diffusion and the vertical height were conducted, and the average value was calculated. The slurry was stirred for 6 min and measured again to complete the test.

The initial and final setting times of the prepared RRM were determined according to International Standard ISO 9597-2008 “Cement-Test methods-Determination of setting time and soundness, NEQ”^[27]. The mortar was mixed and blended to a workable consistency. A Vicat apparatus was then used to perform needle penetrations at fresh locations for each measurement. The initial and final setting times were taken as the elapsed time required to achieve a penetration of 4 ± 1 and 0.5 mm, respectively.

The chemical compositions of raw materials and WCSA were characterized by x-ray fluorescence spectrometry (XRF; Spectro XEPOS 05C, SPECTRO, Germany). The mineral phases of the raw materials, WCSA clinkers, and RRM hydration products were characterized by x-ray diffraction (XRD; Rigaku Dmax-2500 PC, Rigaku, Japan) using Cu-Kα radiation with 50 kV voltage, 100 mA current, and a scanning speed of 2.4°/min over a range of 5°–65°. The morphologies and structures of RRM samples were characterized with scanning electron microscopy coupled with an energy-dispersive spectrometer (SEM/EDS; Zeiss Supra 55, Carl Zeiss MERLIN Compact, Germany). The hydrated WCSA samples were characterized using a thermogravimetric analysis combined with the differential scanning calorimetry (TGA/DSC; TGA/DSC 1, Mettler Toledo, Switzerland) under nitrogen atmosphere with a heating rate of 10°C/min from 30°C to 400°C.

TABLE 1 | Mechanical properties of the WCSA mortar.

Compressive strength (MPa)			Flexural strength (MPa)			Setting time (min)	
1 day	3 days	28 days	1 day	3 days	28 days	Initial	Final
41.9	59.9	73.4	7.2	8.0	9.1	20	28

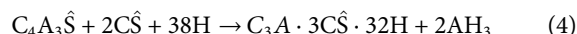
Life cycle assessment (LCA) was conducted using the SimPro ReCiPe2016 H 1.01 model according to ISO 14040 (ISO, 2006). The goal of this LCA study was to appraise the environmental impact of WCSA, CSA, and OPC clinker production chains, and the boundary considered in this study was from the cradle to the gate of the materials' production facility. The processes included mainly raw material transportation, raw material preparation, and production of the three cementitious materials. The function unit for the three techniques was established as 1 ton production of clinker. LCA inventory data were collected for each step in each material's production process. The inventory included mainly inputs of energy and source inputs, and outputs of waste and pollutants. Diesel was used for raw material transportation, and the vehicle used was assumed to be a diesel truck with 28 tons, and the transportation distance of each raw material was assumed to be 50 km from the mining facility or the solid waste facility to the gates of the production facility. Electricity was used mainly for raw material preparation and equipment, and coal was mainly used for material production. Data for raw material consumption, energy consumption, waste, and pollution emission were obtained mainly from industry statistics and literature (Huntzinger and Eatmon, 2009; Li et al., 2014; Li et al., 2019a; Chen et al., 2015; Jeswiet and Szekeres, 2016; Ren et al., 2017b; Ren et al., 2020). Detailed system boundary, function unit, and life cycle inventory are provided in **Supplementary Table S3**.

RESULTS AND DISCUSSION

Physicochemical and Mechanical Properties of WCSA

The main mineral components of WCSA were ye'elimite ($\text{Ca}_4\text{Al}_6\text{O}_{12}\text{SO}_4$, $\text{C}_4\text{A}_3\hat{\text{S}}$), dicalcium silicate (C_2S , mainly α' - C_2S and β - C_2S), and anhydrite (CaSO_4 , $\text{C}\hat{\text{S}}$) (**Supplementary Figure S2**), which were similar to those of ordinary CSA cement (Ren et al., 2020). During the hydration process of WCSA, $\text{C}_4\text{A}_3\hat{\text{S}}$ can quickly react with H_2O and $\text{C}\hat{\text{S}}$ to form ettringite (**Eq. 4**) (Telesca et al., 2014), which can contribute to much of the early-age mechanical strength. C_2S can also react with H_2O to form C-S-H gel (**Eq. 5**) (Li et al., 2019b; Yao et al., 2019), which can contribute to the later strength development. The mechanical properties of the WCSA mortar are shown in **Table 1**. The prepared WCSA had compressive strengths of 41.9, 59.9, and 73.4 MPa and flexural strengths of 7.2, 8.0, and 9.1 MPa after a curing age of 1 day, 3 days, and 28 days, respectively. The ratio of 3-day compressive strength to 28-day compressive strength was above 0.8, owing to the rapid hydration of the main mineral $\text{C}_4\text{A}_3\hat{\text{S}}$ and the relatively lower hydration reactivity of C_2S (Wang et al., 2016; Li et al., 2019b; Yao et al., 2020). The initial and final

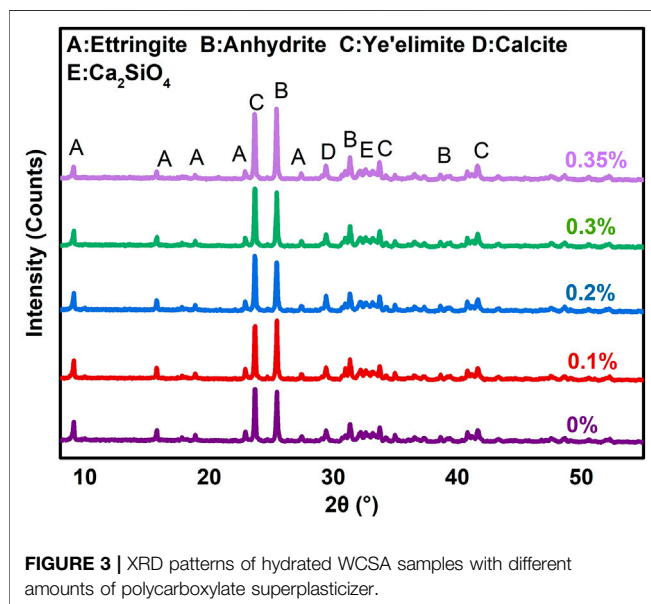
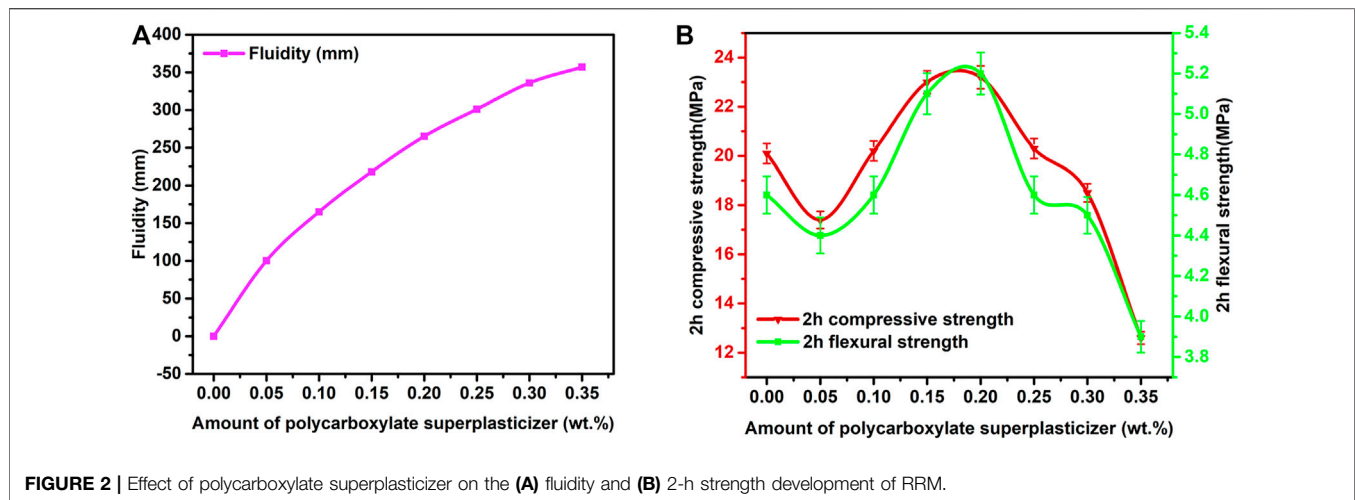
setting times of the WCSA were only 20 and 28 min, respectively. These results indicated high early strength, high later strength, and fast hardening properties of the WCSA, which were suitable for RRM preparation.



Effect of Polycarboxylate Superplasticizer

Polycarboxylate superplasticizer was added into the prepared RRM to adjust its fluidity at a low W/B ratio. The influence of different amounts of polycarboxylate superplasticizer on the fluidity and 2-h strength development of the WCSA-based RRM was studied. As shown in **Figure 2A**, the fluidity of the RRM increased with the increase of the amount of polycarboxylate superplasticizer added. The SEM images of RRM (**Supplementary Figure S3**) indicated that the minerals were more dispersed at 0.2% polycarboxylate superplasticizer than those at 0% polycarboxylate superplasticizer, and more needle-like ettringite was observed. Polycarboxylate superplasticizer preferentially could absorb on aluminate phases that have a positively charge surface and modify the fluidity of the fresh mixture by producing electrostatic repulsion between the anhydrous and hydrated cement particles (Tian et al., 2019; Li et al., 2021), which contributed to the increase of fluidity of RRM with polycarboxylate superplasticizer added. A recent study reported that the use of polycarboxylate superplasticizer did not significantly influence the hydration process of ye'elimite after the main hydration period and could reduce expansion after 4 days of curing (Li et al., 2021). With these effects, this work used polycarboxylate superplasticizer to promote the constructability and durability of the RRM.

The existing literature has shown that the adsorption of polycarboxylate superplasticizer on ettringite could inhibit the growth of ettringite crystals and delay the setting time of CSA cement in the early-age hydration period (Sun et al., 2011; Ma et al., 2014; Su et al., 2019; Li et al., 2021), which may affect the early-age strengths of RRM. In this work, the 2-h compressive and flexural strengths of RRM fluctuated with the addition of polycarboxylate superplasticizer, and the maximum values occurred when the addition amount was 0.2% (**Figure 2B**). However, the overall compressive and flexural strengths of RRM at 2-h hydration age were relatively low and were decreased significantly when the amount of polycarboxylate superplasticizer content was higher than 0.2%. The XRD patterns of hydrated WCSA samples with different amounts of polycarboxylate superplasticizer at 2-h hydration age (**Figure 3**) showed that the main mineral phases of all samples were ettringite, anhydrite, and ye'elimite. When the polycarboxylate superplasticizer was 0.2%, the ettringite peak was the highest and the anhydrite peak was the lowest, indicating the



highest degree of hydration among the samples. The TG/DTG curves (Supplementary Figure S4A) indicated that, with the increasing amounts of added polycarboxylate superplasticizer, the amounts of ettringite first increased and then decreased, which was consistent with the change trend of the 2-h compressive and flexural strengths of RRM.

The above results indicated that a small content of polycarboxylate superplasticizer could increase the fluidity of WCSA effectively. However, excessive polycarboxylate superplasticizer would inhibit the hydration of WCSA and the formation of ettringite, thereby reducing the early-age strength of RRM.

Effect of Lithium Carbonate and Boric Acid

When the amount of added polycarboxylate superplasticizer was set at 0.2%, to deal with the decline of the early-age strength of

RRM caused by polycarboxylate superplasticizer, lithium carbonate was added. The influence of different amounts of lithium carbonate on the initial setting time and 2-h strength development of the WCSA-based RRM is shown in Figure 4. The 2-h compressive and flexural strengths obviously increased with the addition of lithium carbonate and then dropped when the addition amount was over 0.2% (Figure 4A). Correspondingly, the initial setting time of RRM initially decreased and then increased (Figure 4B). The highest 2-h compressive and flexural strengths reached 36.5 and 8.5 MPa, respectively, which were much higher than those without lithium carbonate addition, indicating that lithium carbonate strongly accelerated the early-age hydration of WCSA in RRM.

During the hydration process of RRM, Li^+ introduced by lithium carbonate would induce a fast precipitation of amorphous Li-containing $\text{Al}(\text{OH})_3$ and the consumption of aluminate ions from the solution (Cau Dit Coumes et al., 2017b). Consequently, it would induce a fast dissolution of ye'elimite. Meanwhile, Li-containing $\text{Al}(\text{OH})_3$ would provide seeds for the heterogeneous nucleation of amorphous $\text{Al}(\text{OH})_3$, leading to massive precipitation of hydrates (mainly ettringite) (Cau Dit Coumes et al., 2017b). Therefore, the early-age WCSA hydration was significantly accelerated and the mechanical strengths were quickly increased. However, the acceleration effect of lithium carbonate was not linear with the addition amount. The XRD patterns and TG/DTG curves of hydrated WCSA samples with different amounts of lithium carbonate at 2-h hydration age (Supplementary Figures S4B, S5A) showed that, the ettringite peak intensity was the highest at 0.2% addition amount, rather than increased with the addition amount of lithium carbonate. As shown in Figure 4A, the compressive and flexural strengths decreased when the addition amount exceeded 0.2%. Cau Dit Coumes et al. (2017a) found that, the duration of period of low thermal activity produced by WCSA hydration tended to decrease at higher lithium additions, indicating the lack of sustainability of the acceleration effect induced by excessive lithium carbonate. Parr et al. (2004) also mentioned that the higher the lithium concentration, the faster the hydration of calcium aluminate

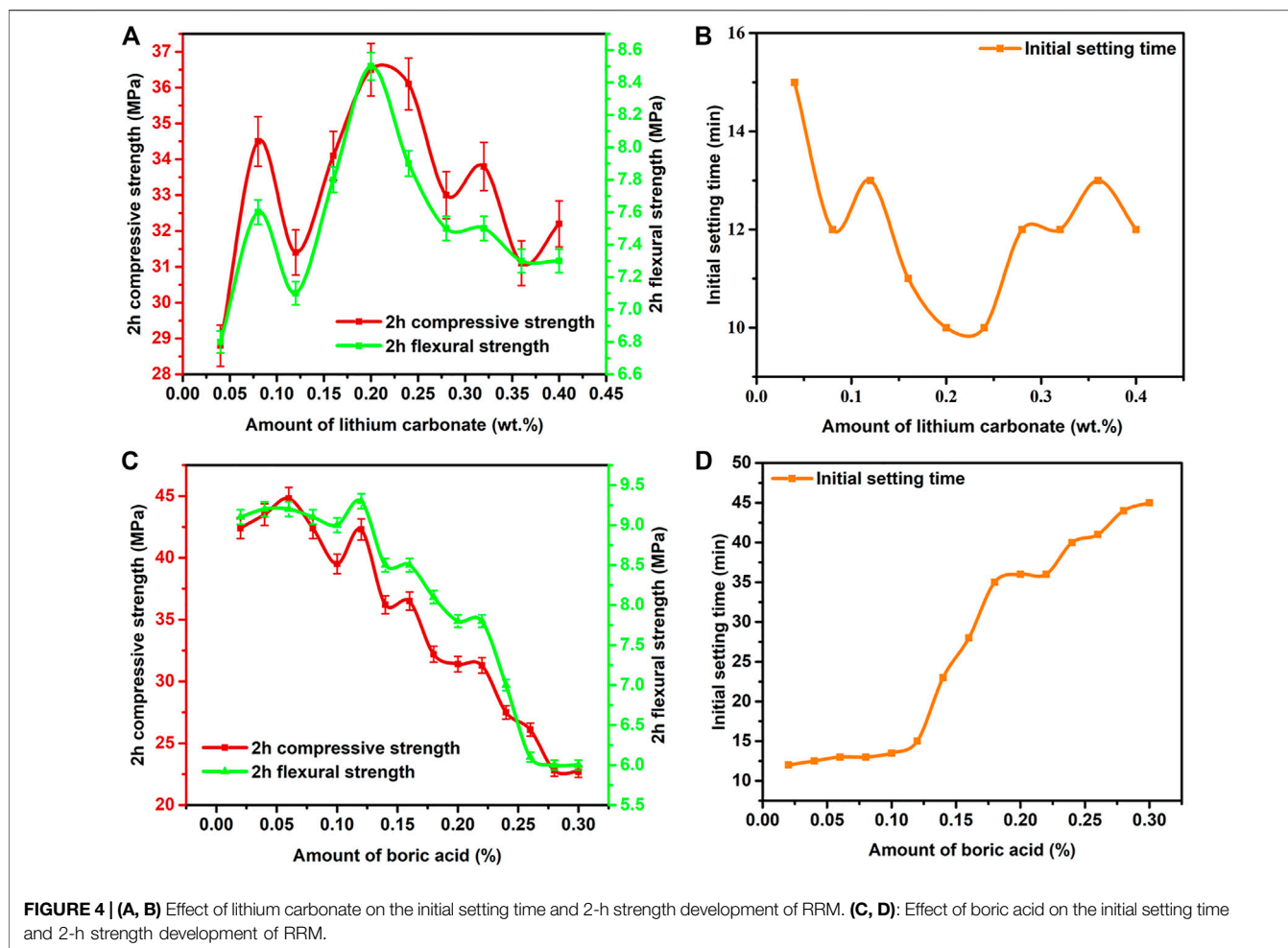


FIGURE 4 | (A, B) Effect of lithium carbonate on the initial setting time and 2-h strength development of RRM. **(C, D):** Effect of boric acid on the initial setting time and 2-h strength development of RRM.

cement until a limit above which a plateau effect occurred. These might explain the limited increase in compressive and flexural strengths induced by excessive lithium carbonate.

The above results indicated that small addition of lithium carbonate could effectively increase the early-age mechanical strengths of RRM and reduce the setting time. However, as shown in **Figure 4B**, the initial setting time was decreased to less than 15 min, which was unfavorable to the actual engineering application of RRM. Borate compound is well known for acting as set retarder during the hardening of cement (Hu et al., 2017; Chen et al., 2019). In this work, boric acid was added to extend the initial setting time of RRM (added 0.2% polycarboxylate superplasticizer and 0.2% lithium carbonate). As shown in **Figures 4C,D**, the initial setting time of RRM was prolonged with the addition of boric acid, but the compressive and flexural strengths decreased quickly as the addition amount increased.

In **Figure 4C**, small addition of boric acid ($\leq 0.06\%$) slightly increased the mechanical strengths of RRM. It might be explained that a small amount of boric acid neutralized OH^- and promoted the release of Li^+ , which accelerated the hydration of RRM. However, a higher amount of boric acid significantly reduced the mechanical strengths of RRM. It has been reported that a poorly crystallized borate compound [ulexite, $\text{NaCaB}_5\text{O}_6(\text{OH})_6\text{A}$

$5\text{H}_2\text{O}$] was formed during the CSA cement hydration, which covered the surface of CSA clinker particles and prevented the further dissolution of ye'elimite, producing a strong retarding effect (Champenois et al., 2015; Chen et al., 2019). The SEM images of RRM (**Figure 5**) showed that, some substances were attached to the surface of the hydration products when 0.16% boric acid was added, indicating the formation of poorly crystallized borate compound. Meanwhile, excessive H^+ in boric acid neutralized OH^- in $\text{Al}(\text{OH})_3$ and inhibited the formation of ettringite. These effects led to the obvious decrease in mechanical strengths of RRM.

When the addition amount of boric acid was 0.16%, the initial setting time was 28 min, which was close to the requirement of ≤ 30 min in JC/T 2381-2016 "Repairing mortar, 2016"^[25]. Meanwhile, the compressive and flexural strengths still reached 36.1 and 8.5 MPa at 0.16% addition amount, respectively. Therefore, 0.16% addition amount of boric acid might be more suitable for the RRM and was chosen in this study.

Effect of Latex Powder

When the addition amount of polycarboxylate superplasticizer, lithium carbonate, and boric acid added were set at 0.2%, 0.2%, and 0.16%, respectively, latex powder was added to increase the

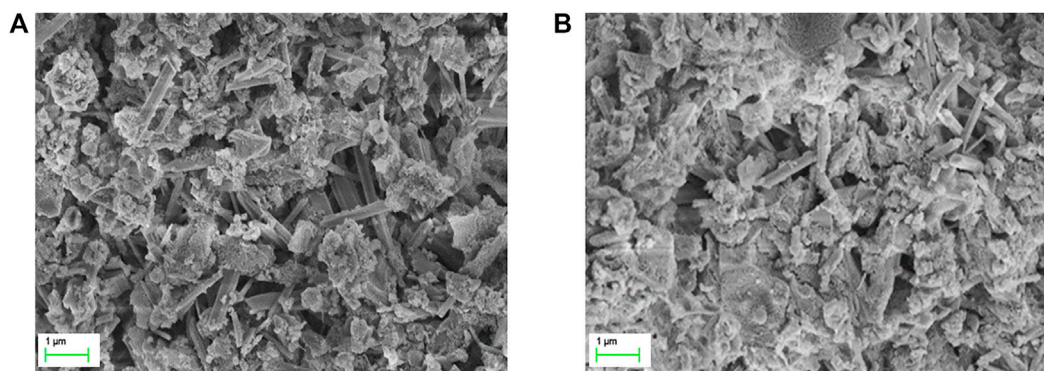


FIGURE 5 | SEM images of RRM: (A) 0% boric acid; (B) 0.16% boric acid.

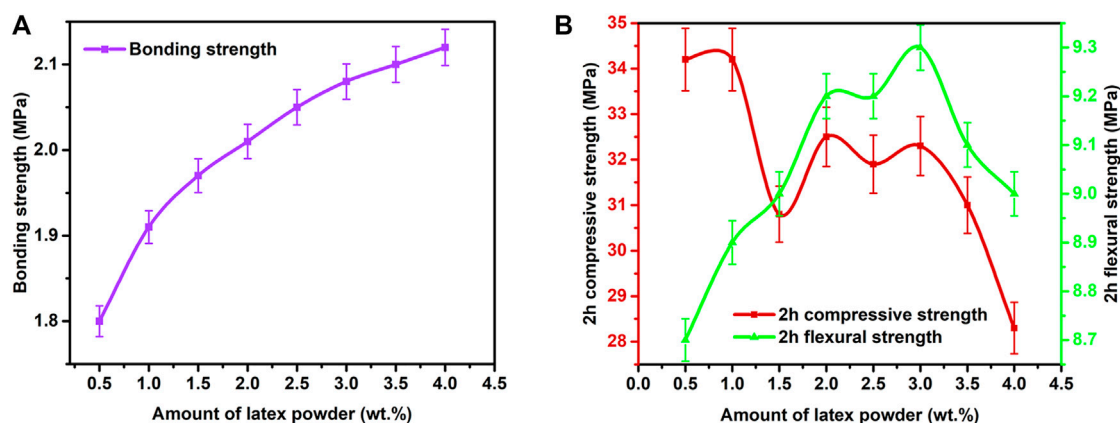


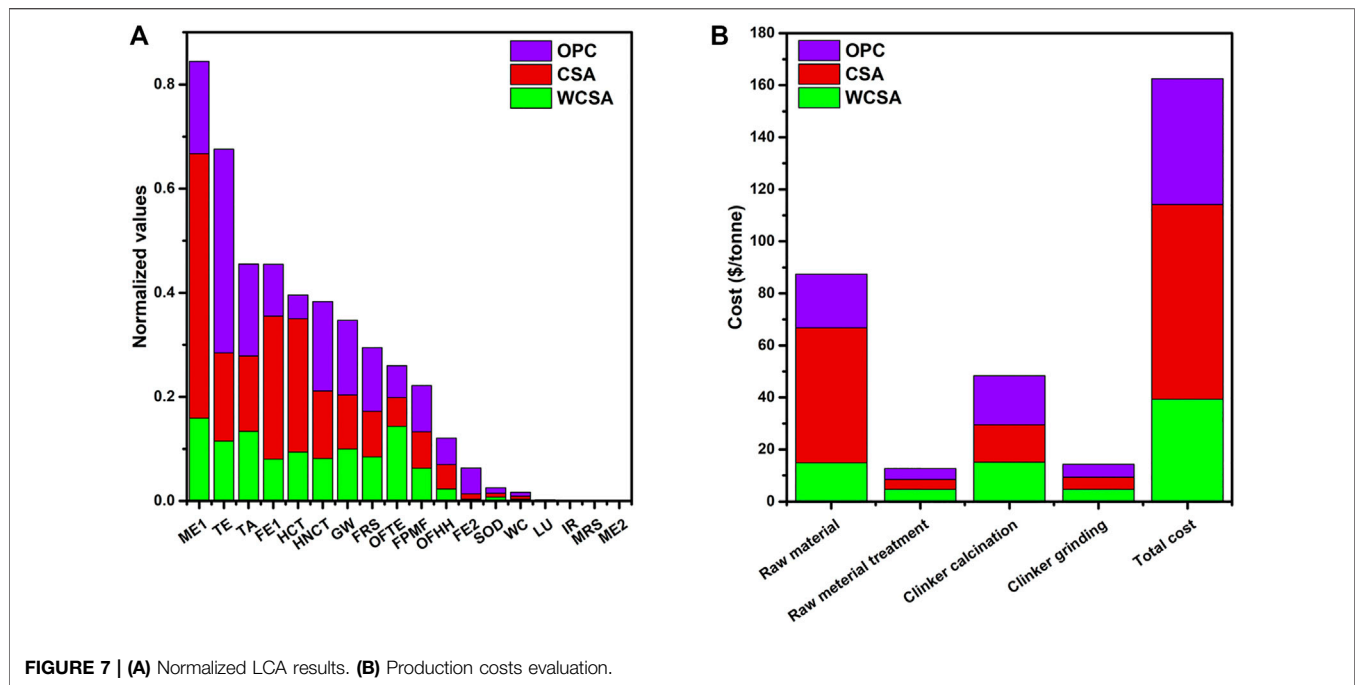
FIGURE 6 | Effects of latex powder on the 1-day bonding strength and 2-h mechanical strengths of RRM.

bonding strength of RRM. Redispersible latex powder could increase the flexural strength and bonding strength of the mortar, but it would reduce the compressive strength (Wang Peiming, 2018; Liu et al., 2019; Fan Chengwen, 2020; Lin et al., 2020). In this work, the influencing effects of latex powder on the 1-day bonding strength and 2-h mechanical strengths of RRM were studied (Figure 6). In the presence of an increased amount of latex powder, the bonding strength and flexural strength of the RRM generally increased; however, the 2-h compressive strength showed an overall downward trend. When the addition amount of latex powder exceeded 3%, the compressive strengths significantly decreased and the flexural strengths also decreased slightly.

The latex powder was able to increase the mortar bonding strength and flexural strength because it could form an emulsion with water and became evenly dispersed in the RRM slurry. The polymer particles distributed in the emulsion then gradually deposited onto the cement particle surfaces during the hydration process. The polymer particles were connected by mutual fusion to form membranes, and they eventually formed a continuous network structure into which the RRM hydrates became intertwined (Wang Peiming, 2018). This process

increased the contact area between the internal RRM particles and played a bridging role to decrease the tensile stress, and it was able to effectively absorb and transmit energy (Fan Chengwen, 2020; Wang Peiming, 2018). As a result, the bonding strength and flexural strength of the RRM was increased. However, the XRD patterns of hydrated WCSA samples with different amounts of latex powder added (Supplementary Figure S5B) showed that the anhydrite peak intensity generally increased when the addition amount increased from 1% to 4%, indicating the inhibitory effect of latex powder on the hydration of WCSA. In addition, Zhao et al. (2019) found that there were enlargement effects of redispersible polymer powders on porosity, average pore diameter, and mean pore diameter of pores in cement mortars. These effects probably led to the reduction of the compressive strength.

When the addition amount of latex powder was 2%, the 1-day bonding strength and 2-h compressive and flexural strength were 2.01, 32.5, and 9.2 MPa, respectively, which were much higher than the requirements for rigid repair mortar in JC/T 2381-2016. After curing age of 1 day, 3 days, and 28 days, the compressive strengths of RRM reached 57.2, 58.6, and 71.8 MPa, and the flexural strengths reached 12.6, 15.3, and 17.7 MPa, respectively. These results indicated



that a high-performance RRM was successfully prepared *via* using solid waste-based CSA cement as binding material, standard sand as aggregate, and four additives as performance modifiers. Collectively, the optimal addition amounts of polycarboxylate superplasticizer, lithium carbonate, boric acid, and latex powder were set at 0.2 wt%, 0.2 wt%, 0.16 wt%, and 2 wt%.

Life Cycle Assessment and Economic Analysis

Both CSA cement and OPC are usually used as the cementing materials for RRM. In order to evaluate the potential environmental benefits of using WCSA to prepare RRM, the LCA analysis of the production of WCSA, CSA cement, and OPC was conducted. The LCA results of 18 environmental impact categories are shown in **Figure 7A**. The LCA results indicated that, the WCSA production had a much lower overall environmental impact than traditional CSA cement and OPC production. It had obvious environmental benefits in the following major categories, i.e., marine ecotoxicity, terrestrial ecotoxicity, freshwater ecotoxicity, human carcinogenic and non-carcinogenic toxicity, and global warming. Previous studies also concluded that the process for preparing WCSA was more environment-friendly than that for producing traditional CSA cement (Ren et al., 2017b; Yao et al., 2019).

(ME1—Marine ecotoxicity; TE—Terrestrial ecotoxicity; TA—Terrestrial acidification; FE1—Freshwater ecotoxicity; HCT—Human carcinogenic toxicity; HNCT—Human non-carcinogenic toxicity; GW—Global warming; FRS—Fossil resource scarcity; OFTE—Ozone formation, Terrestrial ecosystems; FPMF—Fine particulate matter formation; OFHH—Ozone formation, Human health; FE2—Freshwater eutrophication; SOD—Stratospheric ozone depletion; WC—Water consumption;

LU—Land use; IR—Ionizing radiation; MRS—Mineral resource scarcity; ME2—Marine eutrophication.)

The production of WCSA could consume large amounts of industrial solid wastes, reduce the use of high-grade raw materials, and increase the added value of industrial solid wastes. Production costs of WCSA, CSA, and OPC clinkers were also evaluated (**Figure 7B**), and the total production costs for WCSA, CSA, and OPC clinkers were estimated at 39.33\$, 74.78\$, and 48.42\$, respectively (detailed data are provided in **Supplementary Table S4**). The use of industrial solid wastes significantly contributed to the cost reduction for WCSA production. In addition, a comparison of the mechanical properties among WCSA, CSA, and OPC (**Supplementary Table S5**) showed that WCSA had much higher compressive strengths than commercial CSA and OPC with lower cost, especially the early-age strengths of WCSA were two to three times that of OPC. The high early-age strength property of WCSA (i.e., 3-day hydration to achieve 80% of 28-day compressive strength) could effectively reduce the curing time of RRM, thereby improving repair efficiency. Therefore, WCSA obtained better performance at a lower cost and had greater advantages in preparing RRM. These results indicated that the production of WCSA would achieve large-scale utilization of industrial solid wastes and high performance, reducing environmental burden and production cost, which might have the potential to promote the industrial chain development of solid waste-derived high-performance RRM.

CONCLUSION

The prepared RRM exhibited excellent early-age compressive, flexural, and bonding strengths, which were mainly attributed to the high early strength and fast hardening properties of WCSA. In addition, the fluidity, early-age hydration, and mechanical strengths of

RRM were well adjusted and optimized using four additives, including polycarboxylate superplasticizer, lithium carbonate, boric acid, and latex powder.

The polycarboxylate superplasticizer could effectively improve the fluidity of RRM, but it also had an adverse effect on the early-age strength development. As a solution to the above problem, a very small amount of lithium carbonate could significantly improve the early-age hydration and strength development of RRM by promoting the dissolution of ye'elimite and the precipitation of hydrates (mainly ettringite). In addition, adding a small amount of boric acid prolonged the too short setting time of RRM caused by lithium carbonate, with ensuring its high early-age compressive and flexural strengths. Finally, the addition of a certain amount of latex powder could effectively increase the mortar bonding and flexural strengths, and only caused a limited and acceptable decrease in compressive strength.

Collectively, the WCSA production can significantly reduce the consumption of natural resources and production costs, which is more environmental-friendly than that for traditional CSA cement and OPC. This work provides an innovative and promising method for the production of high-performance RRM using WCSA, standard sand, and four suitable additives, which is in line with the current trend towards a circular economy and green sustainable development.

DATA AVAILABILITY STATEMENT

The original contributions presented in the study are included in the article/**Supplementary Material**. Further inquiries can be directed to the corresponding author.

REFERENCES

- Benhelal, E., Zahedi, G., Shamsaei, E., and Bahadori, A. (2013). Global Strategies and Potentials to Curb CO₂ Emissions in Cement Industry. *J. Clean. Prod.* 51, 142–161. doi:10.1016/j.jclepro.2012.10.049
- Cau Dit Coumes, C., Dhoury, M., Champenois, J.-B., Mercier, C., and Damidot, D. (2017a). Combined Effects of Lithium and Borate Ions on the Hydration of Calcium Sulfoaluminate Cement. *Cement Concrete Res.* 97, 50–60. doi:10.1016/j.cemconres.2017.03.006
- Cau Dit Coumes, C., Dhoury, M., Champenois, J.-B., Mercier, C., and Damidot, D. (2017b). Physico-chemical Mechanisms Involved in the Acceleration of the Hydration of Calcium Sulfoaluminate Cement by Lithium Ions. *Cement Concrete Res.* 96, 42–51. doi:10.1016/j.cemconres.2017.03.004
- Cement-Test methods-Determination of strength Cement - Test Methods - Determination of Strength, ISO 679-2009. <https://www.iso.org/standard/4848.html>.
- Cement-Test methods-Determination of setting time and soundness Cement-Test Methods-Determination of Setting Time and Soundness, NEQ, ISO 9597-2008.
- Champenois, J.-B., Dhoury, M., Cau Dit Coumes, C., Mercier, C., Revel, B., Le Bescop, P., et al. (2015). Influence of Sodium Borate on the Early Age Hydration of Calcium Sulfoaluminate Cement. *Cement Concrete Res.* 70, 83–93. doi:10.1016/j.cemconres.2014.12.010
- Chen, W., Hong, J., and Xu, C. (2015). Pollutants Generated by Cement Production in China, Their Impacts, and the Potential for Environmental Improvement. *J. Clean. Prod.* 103, 61–69. doi:10.1016/j.jclepro.2014.04.048
- Chen, W., Ling, X., Li, Q., Yuan, B., Li, B., and Ma, H. (2019). Experimental Evidence on Formation of Ulexite in Sulfoaluminate Cement Paste Mixed with High Concentration Borate Solution and its Retarding Effects. *Construction Building Mater.* 215, 777–785. doi:10.1016/j.conbuildmat.2019.04.242

AUTHOR CONTRIBUTIONS

JL: Investigation, Writing—Original draft, Formal analysis, Data curation, and Visualization. DX: Experimental analysis, Writing—Original draft, Review, and Editing. XW: Supervision, Methodology, and Review. KW: Investigation and Editing. WW: Formal analysis and Funding acquisition.

FUNDING

This work was funded by the National Key R&D Program of China (No. 2020YFC1910000) and the Natural Science Foundation of Shandong Province (CN) Youth Project (No. ZR2020QE201).

ACKNOWLEDGMENTS

We thank the support of the National Engineering Laboratory of Coal-fired Pollutants Emission Reduction (Shandong University).

SUPPLEMENTARY MATERIAL

The Supplementary Material for this article can be found online at: <https://www.frontiersin.org/articles/10.3389/fmats.2021.792299/full#supplementary-material>

- Chinaconcretes, (2020). Production and Market Analysis of Commercial concrete in China's Provinces and Cities in 2019. <http://www.cnrmc.com/news/show.php?itemid=120134>.
- Du, P., Li, X., Zhou, Z., Lu, X., Zhang, X., Xu, D., et al. (2021). Preparation and Properties of Alite-Modified Calcium Sulfoaluminate Cement. *Adv. Cement Res.* 33, 135–143. doi:10.1680/jadcr.19.00092
- Fan Chengwen, B. Y. L. P. (2020). Study on Early Performance of Rapid Hardening Sulphoaluminate Cement-Based Sealing Material. *Hydro-Science Eng.* 000, 30–35.
- Feng, L., Chen, X.-q., Wen, X.-d., Zhang, Z.-y., and Shou, L.-y. (2019). Investigating and Optimizing the Mix Proportion of Sustainable Phosphate-Based Rapid Repairing Material. *Construction Building Mater.* 204, 550–561. doi:10.1016/j.conbuildmat.2019.01.195
- Gartner, E., and Sui, T. (2018). Alternative Cement Clinkers. *Cement Concrete Res.* 114, 27–39. doi:10.1016/j.cemconres.2017.02.002
- Ge, Z., Yuan, H., Sun, R., Zhang, H., Wang, W., and Qi, H. (2020). Use of green Calcium Sulphoaluminate Cement to Prepare Foamed concrete for Road Embankment: A Feasibility Study. *CONSTR BUILD MATER.* 237, 117791. doi:10.1016/j.conbuildmat.2019.117791
- Han, J.-W., Jeon, J.-H., and Park, C.-G. (2015). Mechanical and Permeability Characteristics of Latex-Modified Pre-packed Pavement Repair Concrete as a Function of the Rapid-Set Binder Content. *MATERIALS* 8, 6728–6737. doi:10.3390/ma8105339
- Hu, Y., Li, W., Ma, S., and Shen, X. (2017). Influence of Borax and Citric Acid on the Hydration of Calcium Sulfoaluminate Cement. *Chem. Pap.* 71, 1909–1919. doi:10.1007/s11696-017-0185-9
- Huntzinger, D. N., and Eatmon, T. D. (2009). A Life-Cycle Assessment of Portland Cement Manufacturing: Comparing the Traditional Process with Alternative Technologies. *J. Clean. Prod.* 17, 668–675. doi:10.1016/j.jclepro.2008.04.007
- Huynh, T.-P., Vo, D.-H., and Hwang, C.-L. (2018). Engineering and Durability Properties of Eco-Friendly Mortar Using Cement-free SRF Binder. *Construction Building Mater.* 160, 145–155. doi:10.1016/j.conbuildmat.2017.11.040

- ISO (2006). *ISO/DIS 14040. Environmental Management - Life Cycle Assessment - Principles and Framework*. Brussels, Belgium: International Standard Iso.
- Jeswiet, J., and Szekeres, A. (2016). Energy Consumption in Mining Communion. *Proced. CIRP* 48, 140–145. doi:10.1016/j.procir.2016.03.250
- Juenger, M. C. G., Snellings, R., and Bernal, S. A. (2019). Supplementary Cementitious Materials: New Sources, Characterization, and Performance Insights. *Cement Concrete Res.* 122, 257–273. doi:10.1016/j.cemconres.2019.05.008
- Li, C., Li, J., Telesca, A., Marchon, D., Xu, K., Marroccoli, M., et al. (2021). Effect of Polycarboxylate Ether on the Expansion of Ye'elimite Hydration in the Presence of Anhydrite. *CEMENT CONCRETE RES.* 140. doi:10.1016/j.cemconres.2020.106321
- Li, C., Nie, Z., Cui, S., Gong, X., Wang, Z., and Meng, X. (2014). The Life Cycle Inventory Study of Cement Manufacture in China. *J. Clean. Prod.* 72, 204–211. doi:10.1016/j.jclepro.2014.02.048
- Li, J., Geng, G., Zhang, W., Yu, Y.-S., Shapiro, D. A., and Monteiro, P. J. M. (2019a). The Hydration of β - and α' -H-Dicalcium Silicates: An X-ray Spectromicroscopic Study. *ACS Sustain. Chem. Eng.* 7, 2316–2326. doi:10.1021/acsuschemeng.8b05060
- Li, J., Zhang, W., Li, C., and Monteiro, P. J. M. (2019b). Green concrete Containing Diatomaceous Earth and limestone: Workability, Mechanical Properties, and Life-Cycle Assessment. *J. Clean. Prod.* 223, 662–679. doi:10.1016/j.jclepro.2019.03.077
- Li, J., Zhang, W., Xu, K., and Monteiro, P. J. M. (2020). Fibrillar Calcium Silicate Hydrate Seeds from Hydrated Tricalcium Silicate Lower Cement Demand. *CEMENT CONCRETE RES.* 137, 106195. doi:10.1016/j.cemconres.2020.106195
- Lin, R., Yang, L., Li, S., Li, R., Sheng, X., and Song, G. (2020). Influences of Polymers on the Properties of Cement-Sodium Silicate Grouts with a High Water-Binder Ratio. *J. CERAM. PROCESS RES.* 21, 393–399.
- Liu, G. J., Bai, E. L., Xu, J. Y., and Yang, N. (2019). Mechanical Properties of Carbon Fiber-Reinforced Polymer Concrete with Different Polymer-Cement Ratios. *Materials (Basel)* 12. doi:10.3390/ma12213530
- Long, W. R., Doyle, J. D., Freyne, S. F., and Ramsey, M. A. (2019). Effects of Impure Water Sources on the Early-Age Properties of Calcium Sulfoaluminate (CSA) Cement. *Adv. Civil Eng. Mater.* 8, 20–30. doi:10.1520/acem20180115
- Ma, B., Ma, M., Shen, X., Li, X., and Wu, X. (2014). Compatibility between a Polycarboxylate Superplasticizer and the Belite-Rich Sulfoaluminate Cement: Setting Time and the Hydration Properties. *Construction Building Mater.* 51, 47–54. doi:10.1016/j.conbuildmat.2013.10.028
- Moffatt, E. G., and Thomas, M. D. A. (2017). Performance of Rapid-Repair concrete in an Aggressive marine Environment. *Construction Building Mater.* 132, 478–486. doi:10.1016/j.conbuildmat.2016.12.004
- Parr, C., Simonin, F., Touzo, B., Wöhrmeyer, C., Valdelièvre, B., and Namba, A. (2004). The Impact of Calcium Aluminate Cement Hydration upon the Properties of Refractory Castables. *Proc. TARJ Meet.*, 1–17.
- Phoo-ngernkham, T., Hanjitsuwan, S., Li, L.-y., Damrongwiriyanupap, N., and Chindaprasit, P. (2019). Adhesion Characterisation of Portland Cement concrete and Alkali-Activated Binders. *Adv. Cement Res.* 31, 69–79. doi:10.1680/jadcr.17.00122
- Repairing mortar (2016). *Repairing Mortar, JC/T, 2381-2016*. Beijing, China
- Ren, C., Wang, W., and Li, G. (2017a). Preparation of High-Performance Cementitious Materials from Industrial Solid Waste. *Construction Building Mater.* 152, 39–47. doi:10.1016/j.conbuildmat.2017.06.124
- Ren, C., Wang, W., Mao, Y., Yuan, X., Song, Z., Sun, J., et al. (2017b). Comparative Life Cycle Assessment of Sulfoaluminate Clinker Production Derived from Industrial Solid Wastes and Conventional Raw Materials. *J. Clean. Prod.* 167, 1314–1324. doi:10.1016/j.jclepro.2017.05.184
- Ren, C., Wang, W., Yao, Y., Wu, S., Qamar, S., and Yao, X. (2020). Complementary Use of Industrial Solid Wastes to Produce green Materials and Their Role in CO₂ Reduction. *J. Clean. Prod.* 252, 119840. doi:10.1016/j.jclepro.2019.119840
- Shahzad, Q., Wang, X., Wang, W., Wan, Y., Li, G., Ren, C., et al. (2020). Coordinated Adjustment and Optimization of Setting Time, Flowability, and Mechanical Strength for Construction 3D Printing Material Derived from Solid Waste. *Construction Building Mater.* 259, 119854. doi:10.1016/j.conbuildmat.2020.119854
- Shi, C., Wang, P., Ma, C., Zou, X., and Yang, L. (2021). Effects of SAE and SBR on Properties of Rapid Hardening Repair Mortar. *J. Building Eng.* 35, 102000. doi:10.1016/j.jobe.2020.102000
- Song, Z., Zhang, A., Li, G., Liu, S., and Zhang, J. (2018). Study of Seawater Corrosion Resistance of Ordinary Portland Cement-Calcium Aluminate Cement-gypsum Mortar Containing Slag. *ADV. CEM RES.* 32, 1–24.
- Su, T., Kong, X., Tian, H., and Wang, D. (2019). Effects of Comb-like PCE and Linear Copolymers on Workability and Early Hydration of a Calcium Sulfoaluminate Belite Cement. *Cement Concrete Res.* 123, 105801. doi:10.1016/j.cemconres.2019.105801
- Sun, N., Chang, W., Wang, L., Zhang, J., and Pei, M. (2011). Effects of the Chemical Structure of Polycarboxy-Ether Superplasticizer on its Performance in Sulphoaluminate Cement. *J. Dispersion Sci. Tech.* 32, 795–798. doi:10.1080/01932691.2010.488132
- Telesca, A., Marroccoli, M., Pace, M. L., Tomasulo, M., Valenti, G. L., and Monteiro, P. J. M. (2014). A Hydration Study of Various Calcium Sulfoaluminate Cements. *Cement and Concrete Composites* 53, 224–232. doi:10.1016/j.cemconcomp.2014.07.002
- Test method for fluidity of cement mortar Test Method for Fluidity of Cement Mortar, GB/T, 2419-2005. Beijing, China. Available at: <http://html.rhhz.net/GLJTKJYWB/20130303.htm>.
- Tian, H., Kong, X., Cui, Y., Wang, Q., and Wang, D. (2019). Effects of Polycarboxylate Superplasticizers on Fluidity and Early Hydration in Sulfoaluminate Cement System. *Construction Building Mater.* 228, 116711. doi:10.1016/j.conbuildmat.2019.116711
- Wang Peiming, Z. G. Z. G. (2018). Mechanism of Redispersible Polymer Powder in Cement Mortar. *J. Chin. Ceram. Soc.* 46, 256–262.
- Wang, W., Wang, X., Zhu, J., Wang, P., and Ma, C. (2013). Experimental Investigation and Modeling of Sulfoaluminate Cement Preparation Using Desulfurization Gypsum and Red Mud. *Ind. Eng. Chem. Res.* 52, 1261–1266. doi:10.1021/ie301364c
- Wang, Z., Wang, M., Wen, Z., and Zhang, W. (2016). Progress on Study of Dicalcium Silicate and Low Calcium Cement with Dicalcium Silicate as a Main Mineral Composition. *Mater. Rev.* doi:10.11896/j.issn.1005-023X.2016.01.012
- Yang, S., Yao, X., Li, J., Wang, X., Zhang, C., Wu, S., et al. (2021). Preparation and Properties of Ready-To-Use Low-Density Foamed concrete Derived from Industrial Solid Wastes. *Construction Building Mater.* 287, 122946. doi:10.1016/j.conbuildmat.2021.122946
- Yao, X., Wang, W., Liu, M., Yao, Y., and Wu, S. (2019). Synergistic Use of Industrial Solid Waste Mixtures to Prepare Ready-To-Use Lightweight Porous concrete. *J. Clean. Prod.* 211, 1034–1043. doi:10.1016/j.jclepro.2018.11.252
- Yao, Y., Wang, W., Ge, Z., Ren, C., Yao, X., and Wu, S. (2020). Hydration Study and Characteristic Analysis of a Sulfoaluminate High-Performance Cementitious Material Made with Industrial Solid Wastes. *Cement and Concrete Composites* 112, 103687. doi:10.1016/j.cemconcomp.2020.103687
- Yeung, J. S. K., Yam, M. C. H., and Wong, Y. L. (2019). 1-Year Development Trend of concrete Compressive Strength Using Calcium Sulfoaluminate Cement Blended with OPC, PFA and GGBS. *Construction Building Mater.* 198, 527–536. doi:10.1016/j.conbuildmat.2018.11.182
- Zhang, J., Li, G., Yang, X., Ren, S., and Song, Z. (2018). Study on a High Strength Ternary Blend Containing Calcium Sulfoaluminate Cement/calcium Aluminate Cement/ordinary Portland Cement. *Construction Building Mater.* 191, 544–553. doi:10.1016/j.conbuildmat.2018.10.040
- Zhang, Y., Wang, Y., Li, T., Xiong, Z., and Sun, Y. (2018). Effects of Lithium Carbonate on Performances of Sulphoaluminate Cement-Based Dual Liquid High Water Material and its Mechanisms. *Construction Building Mater.* 161, 374–380. doi:10.1016/j.conbuildmat.2017.11.130
- Zhao, G., Wang, P., and Zhang, G. (2019). Principles of Polymer Film in Tile Adhesive Mortars at Early Ages. *MATER. RES. EXPRESS* 6. doi:10.1088/2053-1591/ab25c2

Conflict of Interest: The authors declare that the research was conducted in the absence of any commercial or financial relationships that could be construed as a potential conflict of interest.

Publisher's Note: All claims expressed in this article are solely those of the authors and do not necessarily represent those of their affiliated organizations, or those of the publisher, the editors, and the reviewers. Any product that may be evaluated in this article, or claim that may be made by its manufacturer, is not guaranteed or endorsed by the publisher.

Copyright © 2021 Li, Xu, Wang, Wang and Wang. This is an open-access article distributed under the terms of the Creative Commons Attribution License (CC BY). The use, distribution or reproduction in other forums is permitted, provided the original author(s) and the copyright owner(s) are credited and that the original publication in this journal is cited, in accordance with accepted academic practice. No use, distribution or reproduction is permitted which does not comply with these terms.